Behavior of Sandwich Beams With Functionally Graded Rubber Core in Three Point Bending

M.R. Doddamani,[1] **S.M. Kulkarni,**[1] **Kishore** [2]
[1]*Department of Mechanical Engineering, National Institute of Technology Karnataka, Surathkal 575 025, India*

[2]*Department of Materials Engineering, Indian Institute of Science, Bangalore, India*

The three-point bending behavior of sandwich beams made up of jute epoxy skins and piecewise linear functionally graded (FG) rubber core reinforced with fly ash filler is investigated. This work studies the influence of the parameters such as weight fraction of fly ash, core to thickness ratio, and orientation of jute on specific bending modulus and strength. The load displacement response of the sandwich is traced to evaluate the specific modulus and strength. FG core samples are prepared by using conventional casting technique and sandwich by hand layup. Presence of gradation is quantified experimentally. Results of bending test indicate that specific modulus and strength are primarily governed by filler content and core to sandwich thickness ratio. FG sandwiches with different gradation configurations (uniform, linear, and piecewise linear) are modeled using finite element analysis (ANSYS 5.4) to evaluate specific strength which is subsequently compared with the experimental results and the best gradation configuration is presented. POLYM. COMPOS., 32:1541–1551, 2011. © 2011 Society of Plastics Engineers

INTRODUCTION

For flexural loading situations, a structure that has attracted the attention of design engineers is the sandwiches. A rapid development in polymer matrix composites has offered one of the best choices as regards to the possible design innovations for sandwiches. These are composed of two stiff, strong and thin faces (skins) bonded to a light, thick weaker core. Faces sustain in-plane and bending loads, while the core resists transverse shear forces by keeping the facings in place [1]. Sandwiches provide increased flexural rigidity and strength by virtue of their geometry [2–5]. Factors coming under the broad spectrum of microscopical, compositional, and/or chemical structure are known to influence the mechanical

properties [6–9]. Hence, they need to be considered in any new development involving sandwich structures. These systems with a gradient core could open up new avenues as regards to applications. Thus, any further enhancement of sandwich structural performance for critical applications should potentially include new ideas without compromising existing benefits. This can be potentially accomplished by incorporating novel material construction concepts as well as newer class of materials for the face sheets and the core [10]. Hence, a sandwich having a core of functionally graded material (FGM) is taken up for the analysis. To support the need to adopt such a route, in literature gradient syntactic foams where variation of glass hollow spherical microballoons in an epoxy matrix from 43.9 to 25.9 in volume % of the balloons in sliced sections resulted in enhancement of tensile strength and moduli from 23.8 to 41.9 MPa and 2 to 2.47 GPa, respectively [11]. In syntactic foams, by maintaining the volume fraction of all microballoons constant at 60% and selecting different types of microballoons, compressive strength, and energy absorption values vary based on structure of the layers [12]. In another case, compression properties of functionally graded (FG) syntactic foams are studied after establishing gradation using microballoon wall thickness [13].

In recent years, FGMs have gained considerable attention as a potential structural material for future high-speed spacecraft and power generation industries [14]. These are special type of systems where composition and microstructure vary with geometry resulting in change in material property [15, 16]. FGMs are used in applications such as thermal-barriers [17]. As many of the polymeric systems used for developing FGMs are generally associated with the tag of expensiveness, it is decided to examine the gradation in composition and its subsequent behavior under bending when an abundantly available lower density possessing fly ash is used as filler material for the core. Fly ash is a fine particulate waste product derived during generation of power in a thermal power plant. These are inexpensive, possess good mechanical properties and have aspect ratios closer to unity thereby are

expected to display near isotropic characteristics. When used with well-established matrix systems, these help in reducing the cost and either retain or improve desirable and specific mechanical properties. Fly ash has attracted interest [18, 19] lately because of the abundance in terms of volume of the material generated and the environmental-linked problems in the subsequent disposal. Fly ash mainly consists of alumina and silica which are expected to improve the composite properties. It also consist hollow spherical particles (termed as cenospheres [20, 21]), which aid in maintaining lower density values for the composite. This feature is of considerable significance in weight specific applications. As the fillers are of near spherical shape, the resin spread is better. Developing newer and utilitarian systems using ashes which display near isotropic properties should be an interesting and challenging task [22]. In recent years, there is growing interest in the use of natural fibers as reinforcing components for thermo plastics and thermosets. The growing interest in natural fibers is mainly due to their economical production with few requirements for equipment and low specific weight, which results in a higher specific strength and stiffness when compared with synthetic fibers composites. Also, they offer safer handling and working conditions compared with synthetic fibers [23]. In this regard, instead of well-explored man-made fibers (like glass, carbon, aramid, etc.) for the skins, a fairly strong naturally occurring material "jute fiber" is used. This is known for its inexpensiveness. Jute reinforced plastics offer attractive propositions for cost-effective applications [24, 25]. These in the form of laminates have much better properties than their neat resin counterparts [26–30]. Better properties of woven jute fabric reinforced composites have demonstrated their potential for use in a number of consumable goods [25]. Substantial increase in flexural modulus and strength with small amount of reinforcement of unidirectional jute has been reported in the earlier works performed by Kishore and coworkers. [31]. Mohan et al. [24, 31] reported that jute provided a reasonable core material in jute-glass hybrid laminates. They evaluated compressive and flexural properties of the jute-glass reinforced epoxy laminates fabricated by filament winding technique using flat mandrel [24, 31]. Four different hybrid combinations are studied with different glass fiber volume fractions and the results are compared with jute reinforced plastic. They found substantial increase in flexural and compressive properties with hybridization.

For fabricating both the skins and core, a matrix system is required. A thermosetting epoxy is chosen for this purpose. The gradation in core is achieved through natural differential sedimentation at different depths using three kinds of ash particles. Lightweight cenospheres are at the top, heavier particles at the bottom and plerospheres settling between. The ash particles possessing different morphologies are used to yield a system with a matrix material consisting of rubber. Here again, from the standpoint of cost, availability, and the scarce literature [31–33]

prompted for using natural rubber a naturally occurring elastomeric material as the matrix system.

The flexural behavior of sandwich beams has been studied extensively by many investigators. Original works include Hoff and Mautner [34], Krajcinovic [35, 36], DiTaranto [37], Rao [38], Frostig and Shenhar [39], and others. Other studies of sandwich beams using strength of materials analysis are performed by Teti and Caprino [40] and Johnson and Sims [41]. From the experimental point of view, Lingaiah and Suryanarayana [42] performed three-point and four-point bending tests on sandwich specimens with fiberglass-reinforced plastics and aluminum for the facings and aluminum honeycomb/polyurethane foam for the core. Studies on three-point bend tests have been conducted in either flexural [43, 44] or short beam shear test configurations [45, 46]. An experimental investigation of FG sandwich beams subjected to three-point bending is performed by Avila [47]. Studies on three-point bend tests have been conducted in either flexural [43, 44] or short beam shear test configurations [45, 46, 48]. In addition, fiber reinforced syntactic foams [49–51] and syntactic foam core sandwich composites have also been studied for bending properties [52, 53]. Although much work has been done by many researchers, none of them performed an experimental investigation with sandwich structures with rubber core where large variations of mechanical properties are observed. This article is focused on evaluating specific bending strength and modulus of sandwich beams with FG rubber core.

Hence for this study, sandwich composites made up of fly ash reinforced rubber core and jute epoxy skins are fabricated and tested for three-point bending behavior. Sandwich preparation and testing is done according to designed experiments using L9 orthogonal array (OA) [54, 55]. Specific modulus and strength of sandwiches evaluated from load deflection behavior are statistically analyzed to identify the influencing factors. The study considers three parameters that could influence the bending behavior, namely, weight fraction of fly ash, ratio of core thickness to total thickness (C/H ratio) of sandwich, and finally the orientation of fibers in jute fabric. Furthermore, sandwiches with FG core are modeled and analyzed using finite element analysis (FEA) in structural analysis software (ANSYS 5.4). Three cases of gradation expected in the core, namely, uniform (U), linear (L), and piece-wise linear (PL) are addressed to determine specific strength from FEA. Specific strength values so determined from the analysis are compared with the experimental values, first to validate the PL variation in the core and then to derive additional support for the assumption of prevalence of gradation in prepared samples.

EXPERIMENTAL

Materials

The matrix system consists of Natural latex supplied by Karnataka Forest Development Corporation, Rubber

TABLE 1.	Factors and levels selected for this study.		
Factors Levels	Weight fraction of fly ash (%) (Factor 1)	C/H ratio (Factor 2)	Orientation (°) of jute fabric (Factor 3)
Level 1	20	0.4	0°/90°
Level 2	30	0.6	30°/60°
Level 3	40	0.8	45°/45°

TABLE 2.	Jute layers for different C/H ratios.		
C/H ratio	Core thickness, C (mm)	Number of jute layers below core	Number of jute layers above core	Sandwich thickness, H (mm)
0.4	4	6	6	10
0.6	6	4	4	10
0.8	8	2	2	10

division, Sullia, Karnataka, India. The density of latex is found to be 1,060 kg/m³. The filler, viz., fly ash is obtained from Raichur Thermal Power Plant, Raichur (India). This ASTM class "C" fly ash with bulk density of about 900 kg/m³ is found to consist of a mixture of solid and hollow spheres of assorted sizes. Energy dispersive spectroscopy of the fly ash sample revealed the main constituents to be silica (63%) and alumina (26%) [56].

Plan of the Experiment for Bending Test

Experiments are planned based on L9 OA [54]. Table 1 shows the parameters and values of the levels considered.

Processing

For processing of FG cores, conventional casting technique is used. Fly ash, the filler used for core as emphasized earlier consists of a mixture of solid, hollow, and composite particles possessing different densities resembling spherical form to a larger degree. The gradation in the core is expected due to differential settling of these particles. A measured quantity of natural latex is mixed with preweighed amounts of fly ash, sulfur (vulcanizer), and zinc oxide (catalyst) [57] by gentle stirring for about 1 h. The mold used for preparation of core specimen (258 mm × 68 mm × 10 mm) is completely covered on all sides with teflon sheet. Initially silicone releasing agent is applied to the mold to facilitate ease of removal of the cast sample. The mixture is then slowly decanted into the mold cavity followed by curing at 90°C in an oven for about 5–6 h. This procedure is performed for all samples having 20%, 30%, and 40% fly ash by weight. Finally, the cured core sample is removed from the mold and the edges are trimmed.

As regards the sandwich skins, a bi-directional woven jute fabric procured from M/S Barde Agencies, Belgaum (Karnataka) is used. This fabric is cut into layers of dimensions 255 mm × 65 mm in required orientation. Thickness of each fabric piece is 0.5 mm. All the layers of jute fabric are heated in an oven at 70°C for 5–10 min to remove the moisture present. Based on required C/H ratio number of fabric layers to be used are determined (Table 2).

The required number of fabric pieces are dipped in a mixture of epoxy and K-6 hardener and placed on base plate forming the bottom stack of the sandwich. FG cores prepared by earlier mentioned procedure are dipped in resin mixture and placed on the bottom stack of skins. Finally, remaining layers of jute fabrics are stacked to constitute the top stack of skins. A procedure of this nature helps in ensuring a greater degree of spread of the resin on the fibrillar jute. Following this, the excess resin is removed by squeezing operation that is done by tightening of top plate of the mold. The mold assembly is then cured at room temperature for about 24–26 h. The sandwich sample is withdrawn from the mold and trimmed to the required size. Similarly, number of samples is made with various core thickness and skin orientations as presented in Fig. 1. Table 3 presents sample coding used for sandwich samples.

Testing Core for Gradation in Fly Ash Content

Presence of gradation in prepared samples could be established as follows. A test slab of 10 mm × 10 mm × 10 mm is cut from the core sample (Fig. 2a). This is further cut into four thinner slices of dimensions 10 mm × 10 mm × 2.5 mm (Fig. 2b).

Another casting of rubber but without fly ash and having identical measurement is made. It is also sliced. The

FIG. 1.   Geometrical parameters of sandwich [Color figure can be viewed in the online issue, which is available at wileyonlinelibrary.com].

TABLE 3. Sample coding for sandwich specimens.

Sample code	Description
$W_a R_b O_c$	Sandwich specification
W	Indicates factor 1 (Weight % of fly ash)
a	Levels of factor 1 in % (20,30,40)
R	Indicates factor 2 (C/H ratio)
b	Levels of factor 2 (0.4,0.6,0.8)
O	Indicates factor 3 (Jute skin orientation)
c	Levels of factor 3 (0°/90°,30°/60°,45°/45°)

FIG. 3. Sandwich sample mounted on flexural test set-up [Color figure can be viewed in the online issue, which is available at wileyonlinelibrary.com].

weights recorded in two cases are used to establish the content of filler. The weight % of fly ash in each slice could be estimated using the relation,

$$\% \text{ weight of fly ash in slice} = \{[\text{FG core slice weight (g)} \\ - \text{slice weight of pure rubber (g)}]/ \\ \text{weight of FG core slice (g)}\} \times 100 \quad (1)$$

Test for Bending Properties

The three point bending test is performed in accordance with ASTM C 393 [58] using Instron universal testing machine of model 4206 with loading capacity ranging from 0.1 N to 150 kN. Figure 3 shows the sandwich sample mounted on flexural test set-up. The thickness to span ratio of the tested sandwich samples is 1:20. Testing progress is depicted by Fig. 4. The crosshead displacement rate is maintained at 2 mm/min. The load deflection data is recorded at equal intervals up to a point at which the specimen shows the first sign of failure. From load deflection data, bending modulus and strength are estimated using relations (2) and (3), respectively, and the mean of five samples in each sandwich configuration is used for inference.

$$\text{Specific modulus} = E/\rho g \quad (2)$$

$$\text{Specific strength} = 6 \, (FL/4)/BH^3 \rho g \quad (3)$$

where E = bending modulus, F = peak load (N), L = span length (m), B = width of sandwich beam (m), H = thickness of sandwich beam (m), and ρg = weight den-
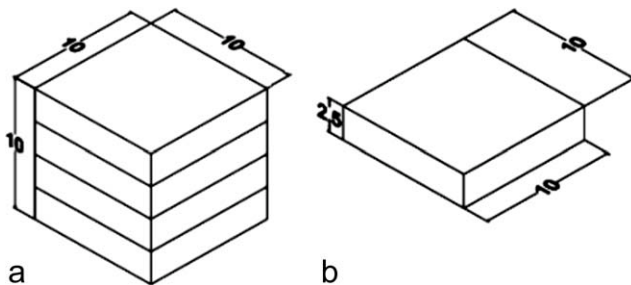
sity. Experimentally measured densities of sandwiches are presented in Table 4.

Flexural test is conducted for two configurations of the sample namely, one with rubber-rich region being upwards and the other in which the ash-rich region is in top position. The analysis of test results (specific modulus and strength) is performed using ANOVA in statistical software MINITAB to identify the most influential factor [59].

FINITE ELEMENT SIMULATION FOR FLEXURAL STRENGTH

Sandwiches with FG core are modeled in FEA package ANSYS 5.4 [17] to estimate specific strength. Fly ash distributions taken into account for uniform configuration are 20%, 30%, and 40% through the thickness. For these weight fractions Young's modulus is estimated using Guth [60] equation which is written as,

$$E_c = E_m \left(1 + 0.67 \, \alpha \, \phi + 1.62 \left(\alpha \, \phi^2\right)\right) \quad (4)$$

where, E_c = Young's modulus of composite, E_m = Young's modulus of matrix, $\alpha = 1$ (shape factor), ϕ = is the volume fraction of filler.

Density values are obtained by using rule of mixtures. While for piecewise linear configuration Young's modulus is obtained by using following relation [61].

$$E_c(z) = E_m + (E_f - E_m) \left(\frac{2 \, z + h}{2 \, h}\right)^k \quad (5)$$

where, E_c = Young's modulus of composite, E_f = Young's modulus of filler, E_m = Young's modulus of matrix, h = height (thickness) of the core, z = 1.25, 3.75, 6.25, and 8.75 corresponding to four notional layers, k =

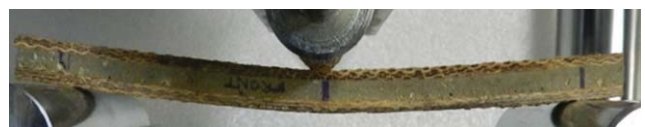FIG. 2. (a) FGM sample and (b) slice cut from sample.

FIG. 4. Test in progress [Color figure can be viewed in the online issue, which is available at wileyonlinelibrary.com].

TABLE 4. Density of sandwiches.

Sandwich code	Density (Kg/m^3)
$W_{20}R_{0.4}O_0$	1,329.5
$W_{20}R_{0.6}O_{30}$	1,334.5
$W_{20}R_{0.8}O_{45}$	1,347.3
$W_{30}R_{0.4}O_{30}$	1,463.2
$W_{30}R_{0.6}O_{45}$	1,433.9
$W_{30}R_{0.8}O_0$	1,468.2
$W_{40}R_{0.4}O_{45}$	1,549.7
$W_{40}R_{0.6}O_0$	1,596.9
$W_{40}R_{0.8}O_{30}$	1,562.6

power law index that takes value greater than or equal to zero and m and f stands for matrix and filler constituents, respectively.

Young's modulus of composite E_c varies continuously in thickness direction (z axis direction—through the thickness) according to power law form. Density values are obtained by water immersion technique for slices of the samples which are used for gradation testing as emphasized before. In case of linear gradation, averaged values two middle layers of PL gradation are considered for both Young's modulus and density.

For skins, Young's modulus is estimated by preparing five tensile samples of jute/epoxy with orientations of $0°/90°$, $30°/60°$, and $45°/45°$ which are subsequently tested as per ASTM [62] guidelines. Density of skins is

calculated through experimental route using formula as outlined in ASTM D792 [63]. Table 5 presents properties of core and skin used in the analysis. Three different gradations of filler U, L, and PL (Fig. 5) are considered during modeling of FG cores. Young's modulus and density of FG cores calculated for different weight fractions of fly ash from constituent properties are provided as input to FEA (Table 5).

For FEA model, gradation in Young's modulus could be taken as analogous to spring element as shown in Fig. 5. The sandwich beams are modeled under three-point loading configurations. A two-dimensional solid element PLANE42 is applied to mesh the model with 2,121 nodes and 2,000 elements. Element edge length is taken as 0.5. The boundary conditions applied to the model are shown in Fig. 6. At the contact surfaces of the layers and between layers and faces of sandwich glue conditions are applied to eliminate relative movement of layers with respect of each other. Furthermore, nodes are merged at the interface allowing proper coupling between layers and interfaces.

RESULTS AND DISCUSSION

Gradation Characterization

Figure 7 presents results obtained from experimental test for gradation characterization. Values in the bracket

TABLE 5. Core and skin properties used in FEA.

	FG Core						
	Young's modulus (GPa)			Density (Kg/m^3)			
Weight % of fly ash	U	L	PL[a]	U	L	PL[a]	Element
20%	0.7575	0.65 (upper), 0.75 (middle), 0.88 (bottom)	0.65 (L1) 0.71 (L2) 0.79 (L3) 0.88 (L4)	1,046.9	1,043.6 (L1), 1,045.9 (L2), 1,047.4 (L3), 1,051.3 (L4)	1,043.6 (L1) 1,045.9 (L2) 1,047.1 (L3) 1,051.3 (L4)	2D Plane 42
30%	0.89	0.68 (upper), 0.865 (middle), 1.15 (bottom)	0.68 (L1) 0.79 (L2) 0.94 (L3) 1.15 (L4)	1,050	1,044.7 (L1), 1,047.1 (L2), 1,050.5 (L3), 1,056.3 (L4)	1,044.7 (L1) 1,047.1 (L2) 1,052.3 (L3) 1,056.3 (L4)	
40%	1.1	0.71 (upper), 1.015 (middle), 1.66 (bottom)	0.71 (L1) 0.88 (L2) 1.15 (L3) 1.66 (L4)	1,053	1,045.9 (L1), 1,051.3 (L2), 1,052.7 (L3), 1,059.6 (L4)	1,045.9 (L1) 1,051.3 (L2) 1,056.3 (L3) 1,059.6 (L4)	

Jute/epoxy skin			
Orientation	E_x (GPa)	E_y (GPa)	Density (Kg/m^3)
$0°/90°$	3.25	2.5	1468
$30°/60°$	1.63	1.25	1451.2
$45°/45°$	2.29	1.77	1444.3

[a] L1-top layer (rubber rich), L4-bottom layer (ash rich).
L: layer.
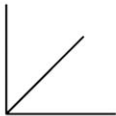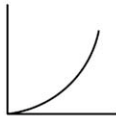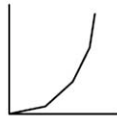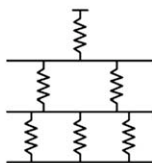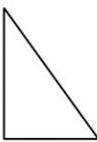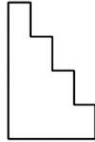
FIG. 5. FG rubber core configurations used in FEA.

represent expected weight % of ash with PL variation in samples of 20%, 30%, and 40% filler content.

As seen from Fig. 7, distribution of fly ash in different slices clearly validates the presence of piecewise linear gradation of fly ash along the thickness in core samples. The gradience in the core helps to achieve a behavior where deflection is more in the initial loading condition and decreases with respect to the magnitude of load applied. This helps in getting more rigidity at loads of higher magnitudes. Furthermore, as the FG core is of particulate composite type, its properties are isotropic taking into account of couplings if there are any.

Specific Bending Modulus

The load and corresponding deflection data (Fig. 8) is noted at equal intervals up to a maximum load at which the specimen shows the first sign of failure (point "A"). The load and deflections obtained during testing are plotted. A typical load deflection curve is shown in Fig. 8.

The load-displacement curves are plotted for all sandwich samples. These consist of an initial linear part followed by a nonlinear portion (Fig. 8). A nonlinear mechanics of materials analysis that accounts for the combined effect of the nonlinear behavior of the facings and core materials (material nonlinearity) and the large deflections of the beam (geometric nonlinearity) are observed. The nonlinear load-deflection behavior of the beams is attributed to the combined effect of material and geometric nonlinearity. The material nonlinearity of the sandwich beam is due to the nonlinear normal stress-strain behavior of the facing material and the FG core. For long beam

spans, even though there is a geometric nonlinearity effect, the overall load-deflection curve of the beam does not deviate much from linearity. For long beam spans, the nonlinearity of the load-deflection curve is mainly due to the combined effect of the facings nonlinearity and the large deflections of the beam. Both effects, however, have a small contribution to the load-deflection behavior, which shows a small deviation from linearity. Some of the general observations made are listed below (Fig. 8).

(1) The load decreases sharply after the end of the elastic region due to failure initiation in sandwich composites (A to B).
(2) All samples have shown small linear region (B to C) before skin failure in compressive side.
(3) Variation in displacement value at which peak load is observed for various types of FG sandwiches is considerable.
(4) The failure originates on the tensile side.

From load deflection data, the average specific strength and specific modulus for five samples (Table 6) are estimated using *Eqs. 2* and *3*.

It can be clearly seen from the table that, rubber up configuration registered higher results compared to ash up
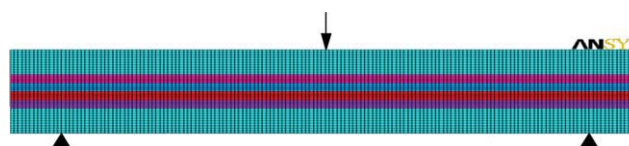

FIG. 6. FEA model of sandwich specimen [Color figure can be viewed in the online issue, which is available at wileyonlinelibrary.com].
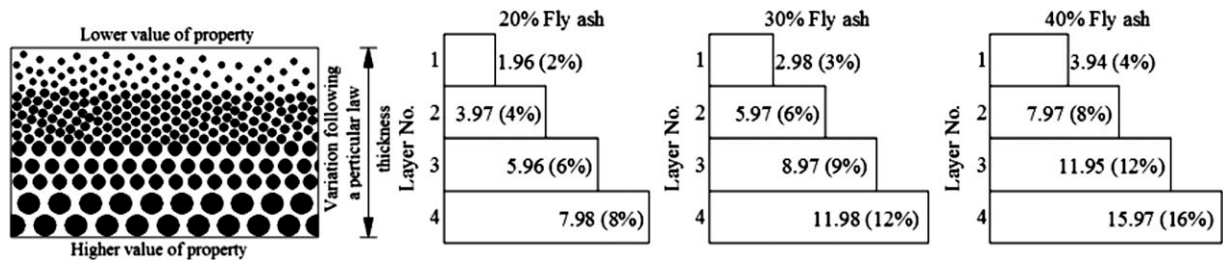
FIG. 7. Distribution of fly ash in different slices of FG core (wt%).

condition for both the properties in the range of 7 to 30%. Figure 9 shows the signal to noise (SN) response plot for specific bending modulus with respect to the parameters under study. SN ratio is the ratio of mean and standard deviation. It indicates the strength of mean with respect to spread of data. This feature makes SN ratio to be more effective in interpreting the results compared with mean values alone.

From the data analysis, vide response Table 7, it is seen that C/H ratio and fly ash % exhibit greater influence compared with the orientation. It is further observed from the table and Fig. 9 that samples with fly ash content of 20%, C/H of 0.8 and an orientation of $0°/90°$ possess highest specific modulus. This could be due to higher C/H ratio implying larger rubber rich region imparting higher modulus to sandwich system.

Specific Bending Strength

Results in Table 6 are used to rank the variables as presented in Table 8.

From SN response table, it can be seen that specific bending strength behavior is prominently governed by fly ash weight % followed by orientation and C/H ratio. From SN response plot shown in Fig. 10, the best combination for specific strength is a sample with fly ash content of 40%, C/H of 0.4 and orientation of $0°/90°$. Reasons for this could be stiffening effect due to high modulus filler and larger skin-epoxy component for lower C/H
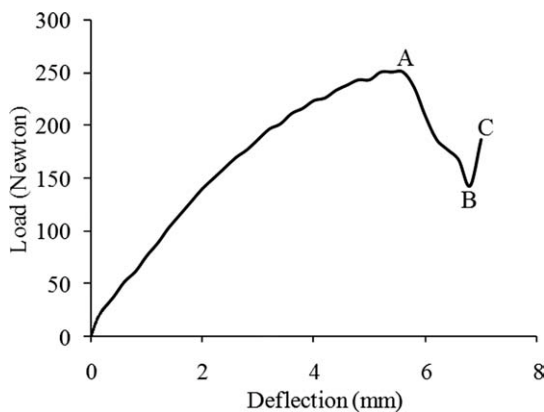

FIG. 8. Typical load-deflection behavior.

ratios. Similar results are obtained for ash up configuration.

Even though $W_{20}R_{0.8}O_{45}$ and $W_{40}R_{0.6}O_0$ are showing higher values (Table 6) for modulus and strength, respectively, inference on basis of these will not lead to an appropriate conclusion. The reason being these values are merely based on average of means. Inference on the grounds of SN analysis leads to a meaningful conclusion as it takes means and data spread into account. By the SN ratio analysis the best sandwich configurations are $W_{20}R_{0.8}O_0$ and $W_{40}R_{0.4}O_0$ for specific modulus and strength, respectively.

Failure Analysis

Within the elastic region of the load-displacement curve (Fig. 8), where no damage is induced, the responses of all specimens to the applied loads are quite similar. This is visible in the form of nearly constant slope in the elastic region of the load-displacement curves. It is observed that the failure starts in the form of crack origination on the tensile side of the specimen as displacement increases. On further loading, the skin of the sandwich composite that is on the tensile side tends to fracture, causing the final failure of the specimen. However, it is not significant enough to lead to the final failure of the specimen. It is observed that the entire specimen fractures at a much later instant of skin fracture. Appearance of small linear region (B to C in Fig. 8) at the end in the load-displacement curves is due to stiffening of FG core before final failure. During the loading process, deformation also takes place in the compression side of the specimen. Cracks initiate from the tensile side and propagate to the compressive side within the core in all sandwich structure specimens.

It is worth discussing the mode of failure. Sandwich samples tested under bending did not display the distinct separation into pieces at failure. The FG core being compliant is observed to be successfully absorbing media. Basically two types of failure mechanisms observed are skin cracking and delamination between skins and core. Figure 11 shows the failed sandwich specimens with their failure modes. The sandwich beams failed at the center of the two supporting rollers. In this portion of the beam, the shear force is zero and only the pure bending exists.

TABLE 6. Specific bending modulus and strength for rubber up and ash up configurations.

| Sandwi-ch coding	Sp. flexural modulus (MPa/Nm^{-1})				Sp. flexural strength (MPa/Nm^{-1})			
	Rubber up	Avg.	Ash up	Avg.	Rubber up	Avg.	Ash up	Avg.
$W_{20}R_{0.4}O_0$	3,945.23	3,953.07	3,410.9	3,410.29	132.7	128.1	103.55	98.81
	3,933.7		3,404.2		128.1		105.32	
	3,961.5		3,419.16		127.7		95.47	
	3,963.7		3,416.4		128.1		99.1	
	3,961.2		3,400.8		123.9		90.61	
$W_{20}R_{0.6}O_{30}$	5,322.6	5,319.4	4,540.15	4,545.36	85.3	88.1	72.3	70.7
	5,306.8		4,545.39		88.1		70.7	
	5,321.3		4,539.4		83.5		71.9	
	5,322.9		4,544.95		92.4		70.7	
	5,323.4		4,556.9		91.2		67.9	
$W_{20}R_{0.8}O_{45}$	7,391.4	7,387.91	6,150.4	6,155.14	54.59	54.59	45.23	48.75
	7,387.91		6,160.73		54.5		50.4	
	7,377.4		6,155.14		57.7		47.9	
	7,393.4		6,155.14		58.1		46.8	
	7,389.42		6,154.28		48.06		53.42	
$W_{30}R_{0.4}O_{30}$	2,996.2	3,001.3	2,390.31	2,398.92	141.4	141.4	115.43	113.26
	3,003.1		2,398.92		141.4		116.23	
	3,004.5		2,398.92		145.5		113.26	
	3,001.3		2,398.92		149.1		111.59	
	3,001.4		2,407.53		129.6		109.79	
$W_{30}R_{0.6}O_{45}$	4,043.3	4,045.36	3,533.59	3,533.57	94.76	101.23	80.17	78.75
	4,047.6		3,528.61		99.14		81.34	
	4,042.4		3,531.75		95.35		75.46	
	4,045.36		3,523.16		106.4		79.1	
	4,048.12		3,550.73		110.5		77.68	
$W_{30}R_{0.8}O_0$	6,559.3	6,562.65	6,018.2	6,018.2	148.7	153.1	120.1	119.3
	6,562.8		6,018.2		149.2		121.3	
	6,570.4		6,018.2		157.3		118.3	
	6,560.55		6,020.9		151.2		121.54	
	6,560.21		6,015.5		159.1		115.26	
$W_{40}R_{0.4}O_{45}$	2,134.3	2,138.92	1,702	1,692.71	149.3	151.4	110.34	117.17
	2,138.69		1,692.67		148.7		121.56	
	2,141.92		1,688.2		152.4		117.17	
	2,139.26		1,690.4		159.3		120.23	
	2,140.42		1,690.3		147.3		116.55	
$W_{40}R_{0.6}O_0$	4,372.5	4,365.98	4,060.12	4,065.98	188.98	192.21	159.21	154.45
	4,370.28		4,068.63		193.5		155.29	
	4,365.39		4,065.98		199.7		152.8	
	4,360.87		4,059.3		191.49		155.7	
	4,360.86		4,075.86		187.38		149.25	
$W_{40}R_{0.8}O_{30}$	6,515.5	6,518.2	6,050.3	6,062.65	155.23	159.53	121.44	125.45
	6,520.7		6,070.4		151.8		123.3	
	6,521.4		6,060.9		161.32		127.56	
	6,518.2		6,058.5		164.2		128.9	
	6,515.2		6,073.15		165.1		126.05	
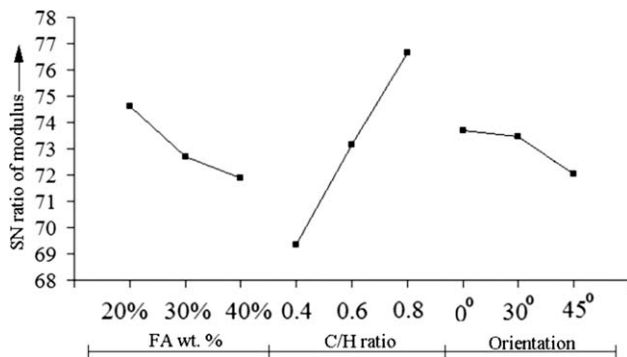
FIG. 9. Response graph of SN ratio of—specific bending modulus (rubber up).

Thus, the sandwich samples are capable of resisting higher bending moment. As the load on the specimen is increased, failures first start under the loads in tensile

TABLE 7. Response of SN ratio—specific bending modulus (rubber up).

	Fly ash weight %	C/H ratio	Orientation
Level 1	**74.61**	69.36	**73.69**
Level 2	72.68	73.15	73.45
Level 3	71.90	**76.66**	72.04
Effect	2.71	7.30	1.66
Rank	2	1	3

TABLE 8. Response of SN ratio—specific bending strength (rubber up).

	Fly ash weight %	C/H ratio	Orientation
Level 1	38.6	**42.92**	**43.84**
Level 2	42.27	41.56	41.99
Level 3	**44.44**	40.83	39.48
Effect	5.85	2.09	4.36
Rank	1	3	2

region and then they propagate toward the compressive zone through compliant FG core.

All the samples failed under skin tension or compression and skin–core debonding. The sandwiches with higher C/H ratio have shown skin–core debonding. FG core takes up most of the load applied for higher C/H ratios (lesser skin thickness). As core is made up of rubber being compliant in nature, relative movements are set up with respect to skin resulting in inter laminar shear stresses. As magnitude of these stresses crosses the adhesive strength delamination creeps in. Some sandwich samples are seen to be intact even after the first sign of failure. These samples exhibited a spring back effect. Samples bearing lower C/H ratio have failed mainly because of skin cracking along the jute orientation. Few samples failed due to shearing at skin-core interface displayed step formation.

Finite Element Analysis

Specific bending strength is estimated by simulating the sample and loading [17] in FEA. Figure 12 represents the plot for bending stress in the sample for one typical loading case. The breaking load taken from experiment is applied on FE model. For this applied load maximum stress (von misses criteria) is recorded and finally, specific strength is determined by taking the ratio of maximum stress to the weight of sample.

The specific strength values obtained from FEA and with experimental approach vide *Eq. 3* is presented in Table 9.
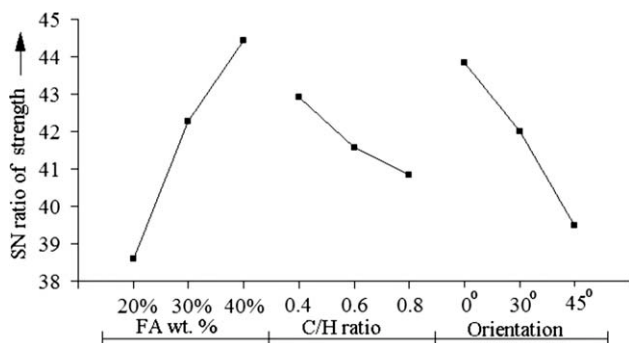

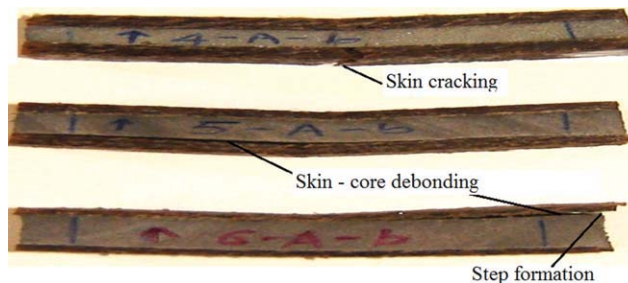FIG. 10. Response graph of SN ratio of—specific bending strength (rubber up).

FIG. 11. Sandwich failure modes [Color figure can be viewed in the online issue, which is available at wileyonlinelibrary.com].
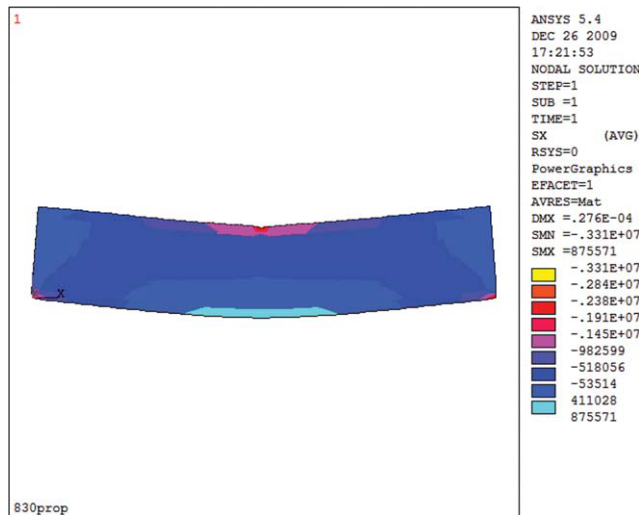

FIG. 12. Bending stress in *x*-direction for typical case [Color figure can be viewed in the online issue, which is available at wileyonlinelibrary. com].

It is significant to note that the experimental results for specific strength match well with FEA values especially for the ones with PL gradation. It is observed that bending strength obtained from FEA is slightly higher than experimental values. This could be due to inability of modeling inhomogenities creeping in during the processing of samples which may result in lowering specific strength.

TABLE 9. Specific strength (MPa/Nm^{-1}) results.

		FEA			
Exp. no.	Sandwich configuration	U	L	PL	Experimental
1	$W_{20}R_{0.4}O_0$	115.4	119.6	132.75	128.1
2	$W_{20}R_{0.6}O_{30}$	78.2	81.5	92.58	88.1
3	$W_{20}R_{0.8}O_{45}$	46.9	48.9	58.58	54.59
4	$W_{30}R_{0.4}O_{30}$	125.1	130.2	147.34	141.4
5	$W_{30}R_{0.6}O_{45}$	84.4	88.8	110.38	101.23
6	$W_{30}R_{0.8}O_0$	129.7	137.6	160.88	153.1
7	$W_{40}R_{0.4}O_{45}$	126.6	131.3	169.11	151.4
8	$W_{40}R_{0.6}O_0$	175.2	179.5	201.42	192.21
9	$W_{40}R_{0.8}O_{30}$	140.2	145.6	165.7	159.53

CONCLUSIONS

Processing and testing of sandwiches with FG core is performed in this work. The gradation in the core is established and quantified physically by weight method. Piecewise linear gradation is modeled in FEA analogous to spring model and results are compared with experimental values.

An experimental investigation of specific bending modulus and strength of sandwich shows that C/H ratio and fly ash weight fraction are the influential factors governing modulus and strength respectively. For specific bending modulus in both cases (i.e., rubber up and ash up, Table 6), $W_{20}R_{0.8}O_0$ registered the best performance while $W_{40}R_{0.4}O_0$ shows better results for specific bending strength.

Specific modulus decreases with an increase in filler content or change of orientation while it increases with C/H ratio. As for specific strength, it increases with an increase in filler content while decrease is recorded with increase in C/H ratio and change of jute orientation. Rubber up configuration registered higher results compared to ash up condition for both modulus (7–27%) and strength (11–30%) properties under study. Increasing fly ash weight fraction decreases bending modulus by 15% and increases bending strength by 29% for rubber up condition.

Finally, validation of the experimental specific bending strength values for rubber up configuration with FE model is highlighted. Strength values estimated from FEA with the assumption of piecewise linear gradation in core match well with experimental results indicating presence of such a gradation.

REFERENCES

1. J. Vinson, *The Behavior of Sandwich Structures of Isotropic and Composite Materials*, Technomic Publishing Company Inc., Pennsylvania (1999).

2. C. Lundsgaard-Larsen, B.F. Sorensen, C. Berggreen, and R.C. Otergaard, in *27th Riso International Symposium on Materials Science*, September 4–7 (2006), Roskilde, Denmark.

3. J.M. Berthelot, *Composite Materials: Mechanical Behavior and Structural Analysis*, Springer Edition, New York (1999).

4. J.A.M. Ferreira and J.D.M. Costa, *J. Cell. Polym.*, **17**, 177 (1998).

5. D. Zenkert, *Handbook of Sandwich Construction*, EMAS Publishing, Chameleon Press Limited, London (1997).

6. M.A. Meyers, P.-Y. Chen, A.Y.-M. Lin, and Y. Seki, *Progr. Mater. Sci.*, **53**, 1 (2008).

7. C.M.R. Dias, H. Savastano Jr., and V.M. John, *Construct. Build. Mater.*, **24**, 140 (2010).

8. V. Cannillo, L. Lusvarghi, C. Siligardi, and A. Sola, *J. Eur. Ceram. Soc.*, **27**, 2393 (2007).

9. L. YongMing, L. ShuQin, C. Jian, W. RuiGang, L. Jian-Qiang, and P. Wei, *Mater. Res. Bull.*, **38**, 69 (2003).

10. M.S. Kirugulige, R. Kitey, and H.V. Tippur, *Compos. Sci. Technol.*, **65**, 1052 (2005).

11. Kishore, R. Shankar, and Sankaran, *Mater. Sci. Eng. A*, **412**, 153 (2005).

12. K. Chittineni and E. Woldesenbet, *J. Eng. Mater. Technol.*, **132**, 295 (2010).

13. N. Gupta and W. Ricci, *Mater. Sci. Eng. A*, **427**, 331 (2006).

14. A.M. Zenkour, *Int. J. Solids Struct.*, **42**, 5224 (2005).

15. S. Mukherjee and G.H. Paulino, *J. Appl. Mech.*, **70**, 359 (2003).

16. V. Cannillo, T. Manfredini, C. Siligardi, and A. Sola, *J. Eur. Ceram. Soc.*, **27**, 1935 (2007).

17. N. Gupta, S.K. Gupta, and B.J. Mueller, *Mater. Sci. Eng. A*, **485**, 439 (2008).

18. S.M. Kulkarni, D. Anuradha, C.R.L. Murthy, and Kishore, *Bull. Mater. Sci.*, **25**, 137 (2002).

19. T.H. Ferrigno, in *Handbook of Fillers and Reinforcements for Plastics*, H.S. Katz and J.V. Milewski, Eds., Van Nostrand Reinhold Co., Chapter 2, New York (1978).

20. R. Mohapatra and J. Rajagopala Rao, *J. Chem. Technol. Biotechnol.*, **76**, 9 (2001).

21. J.W. Pedlow, "Cenospheres," in *Coal Ash Utilization Fly Ash, Bottom Ash, and Slag*, S. Torrey, Ed., Noyes Data Corporation, New Jersey, 353 (1978).

22. S.M. Kulkarni and Kishore, *J. Mater. Sci.*, **37**, 4321 (2002).

23. K. Sabeel Ahmed and S. Vijayarangan, *J. Mater. Process. Technol.*, **207**, 330 (2008).

24. R. Mohan, Kishore, M. K. Shridhar, and R.M.V.G.K. Rao, *J. Mater. Sci. Lett.*, **2**, 99 (1983).

25. M. Jawaid, H. P. S. Abdul Khalil, A. Abu Bakar, and P. Noorunnisa Khanam, *Mater. Des.*, **32**, 1014 (2011).

26. A.N. Shah and S.C. Lakkad, *Fibre Sci. Technol.*, **15**, 41 (1981).

27. M.A. Dweib, B. Hu, A.O. Donnell, H.W. Shenton, and R.P. Wool, *Compos. Struct.*, **63**, 147 (2004).

28. N. Reddy and Y. Yang, *Ind. Crop. Prod.*, **33**, 35 (2011).

29. H. Ku, H. Wang, N. Pattarachaiyakoop, and M. Trada, *Compos. Part B*, **42**, 856 (2011).

30. A.C. Milanese, M.O.H. Cioffi, and H.J.C. Voorwald, *Procedia Eng.*, **10**, 2022 (2011).

31. R. Mohan and Kishore, *J. Reinforc. Plast. Compos.*, **4**, 186 (1985).

32. A. Chakraborty, S. Gopalakrishnan, and J.N. Reddy, *Int. J. Mech. Sci.*, **45**, 519 (2003).

33. N.A. Apetre, B.V. Sankar, and D.R. Ambur, in *44th AIAA Structures, Structural Dynamics and Materials Conference*, April 7–10 (2003), Norfolk, Virginia, USA.

34. N.J. Hoff and S.E. Mautner, *J. Aerospace Sci. Technol.*, **15**, 707 (1948).

35. D. Krajcinovic, *J. Appl. Mech.*, **38**, 773 (1971).

36. D. Krajcinovic, *J. Appl. Mech.*, **42**, 873 (1975).

37. R. A. DiTaranto, *J. Eng. Industry*, **95**, 755 (1973).

38. D.K. Rao, *J. Eng. Industry*, **98**, 391 (1976).

39. Y. Frostig and Y. Shenhar, *Compos. Eng.*, **5**, 405 (1995).

40. R. Teti and G. Caprino, in *First International Conference on Sandwich Construction*, June 19–21 (1989), Stockholm, Sweden.

41. A.E. Johnson and G.D. Sims, *Composites*, **17**, 321 (1986).

42. K. Lingaiah and B. G. Suryanarayana, *Exp. Mech.*, **31**, 1 (1991).

43. R. Maharsia, N. Gupta, and H.D. Jerro, *Mater. Sci. Eng. A*, **417**, 249 (2006).

44. N. Gupta, E. Woldesenbet, and P. Mensah, *Compos. Part A*, **35**, 103 (2004).

45. Kishore, R. Shankar, and S. Sankaran, *J. Appl. Polym. Sci.*, **98**, 673 (2005).

46. Kishore, R. Shankar, and S. Sankaran, *J. Appl. Polym. Sci.*, **98**, 687 (2005).

47. A.F. Avila, *Compos. Struct.*, **81**, 323 (2007).

48. Kishore, R. Shankar, and S. Sankaran, *J. Appl. Polym. Sci.*, **98**, 680 (2005).

49. C.S. Karthikeyan, S. Sankaran, and Kishore, *Polym. Adv. Technol.*, **18**, 254 (2007).

50. C.S. Karthikeyan, S. Sankaran, and Kishore, *Macromol. Mater. Eng.*, **290**, 60 (2005).

51. C.S. Karthikeyan, S. Sankaran, and Kishore, *Polym. Int.*, **49**, 158 (2000).

52. N. Gupta and E. Woldesenbet, *J. Compos. Mater.*, **39**, 2197 (2005).

53. B.V. Sankar, *Compos. Sci. Technol.*, **61**, 689 (2001).

54. D.C. Montgomery, *Design and Analysis of Experiments*, Wiley, New York (2001).

55. P. Ross, *Taguchi Techniques for Quality Engineering*, McGraw-Hill Book Company, New York (1995).

56. Kishore, S.M. Kulkarni, S. Sharathchandra, and D. Sunil, *Polym. Test.*, **21**, 763 (2002).

57. D.C. Blackley, *Polymer Latices: Science and Technology-Application of Lattice*, Chapman & Hall, London (1997).

58. ASTM Standard C 393-00, *"Standard Test Method for Flexural Properties of Sandwich Construction,"* ASTM International (2000).

59. *MINITAB Release 14 User Manual* (2004).

60. E. Guth, *J. Appl. Phys.*, **16**, 20 (1945).

61. G.N. Praveen and J.N. Reddy, *Int. J. Solids Struct.*, **35**, 4457 (1998).

62. ASTM Standard D3039/D3039M-08, *"Standard Test Method for Tensile Properties of Polymer Matrix Composite Materials,"* ASTM International (2008).

63. ASTM Standard D792-08, *"Standard Test Methods for Density and Specific Gravity (Relative Density) of Plastics by Displacement,"* ASTM International (2008).